

# Measurement of normative HDL subfraction cholesterol levels by Gaussian summation analysis of gradient gels

Roy B. Verdery,<sup>1</sup> David F. Benham, Howard L. Baldwin, Andrew P. Goldberg,<sup>2</sup> and Alexander V. Nichols<sup>3</sup>

Department of Medicine, Section on Gerontology and Geriatrics, Bowman Gray School of Medicine, 300 S. Hawthorne Road, Winston-Salem, NC 27103

**Abstract** This report describes development of a computerized method for analyzing polyacrylamide gradient gels of high density lipoproteins (HDL) by Gaussian summation, a simple technique to obtain standardized measurements of size and amount of HDL subfractions. Conditions for reproducibility and ranges of linearity were established. By Gaussian summation analysis, five or six HDL subfractions could be found in the plasma of most normolipidemic people. The relationship of staining intensity to cholesterol level was determined for Coomassie Blue R-250, permitting determination of the cholesterol levels in the individual subfractions, with standard errors of repeated measurements of 2% or less of the total HDL area, and accuracy, limited by the standard error of the chromogenicity, of 1–2 mg/dl for the least abundant fractions and 3–4 mg/dl for the most abundant subfractions. Levels of HDL<sub>2b</sub> measured by this method were statistically the same as levels of HDL<sub>2</sub> measured by dextran sulfate-Mg<sup>2+</sup> precipitation. Gaussian summation analysis of gradient gels was used to measure HDL subfraction cholesterol levels in subjects from the Baltimore Longitudinal Study on Aging to obtain normative levels for men and women for the major HDL subfractions. Comparisons of these levels with each other and with triglyceride and cholesterol levels showed that triglyceride levels were inversely correlated with levels of HDL<sub>2a</sub> and HDL<sub>2b</sub>, cholesterol levels were directly correlated with levels of HDL<sub>3b</sub> and HDL<sub>3a</sub>, and that HDL<sub>3b</sub> levels were inversely correlated with levels of both HDL<sub>2a</sub> and HDL<sub>2b</sub>. — Verdery, R. B., D. F. Benham, H. L. Baldwin, A. P. Goldberg, and A. V. Nichols. Measurement of normative HDL subfraction cholesterol levels by Gaussian summation analysis of gradient gels. *J. Lipid Res.* 1989. 30: 1085–1095.

**Supplementary key words** lipoproteins • Stokes' radius • triglycerides • densitometry • human • sex differences • dextran sulfate

HDL are a heterogeneous mixture of lipoproteins with density  $d$  1.063–1.21 g/ml. This heterogeneity has been appreciated since the 1950s when HDL were shown by analytic ultracentrifugation to have both a main peak, HDL<sub>3</sub>, and a less dense minor peak or shoulder, HDL<sub>2</sub>(1). Levels of HDL<sub>2</sub>, measured by analytic ultracentrifuga-

tion, have been shown to be more closely related to risk for atherosclerosis than total HDL levels or levels of HDL<sub>3</sub> in some studies (2).

HDL subfractions have been studied by several methods including analytic ultracentrifugation (1, 2), polyanion precipitation (3, 4), density gradient ultracentrifugation (5), rate-zonal ultracentrifugation (6), chromatofocusing (7), and polyacrylamide gradient gel electrophoresis (GGE) (8). Of these methods, GGE is singularly amenable for routine measurement of HDL subfractions because it has the highest resolution and many samples can be analyzed simultaneously. GGE can resolve less than 10  $\mu$ g of normal HDL into subfractions varying in Stokes' radius from 4 to 6 nm and differing by less than 0.2 nm (8). GGE can also be used to separate HDL subfractions for composition analysis by immunoblotting (8, 9).

GGE, while widely used for qualitative study of HDL subfractions, has not been standardized to provide quantitative analyses of HDL subfractions comparable from laboratory to laboratory. Different standards have been used to calibrate HDL size; and, even when the same standards have been used, different values for basic physical chemical parameters such as Stokes' radius have been used (8, 10, 11). Although internal standards have been used to estimate levels of HDL subfractions separated by GGE, the relative chromogenicities have not been determined to allow measurement of cholesterol levels in each

Abbreviations: HDL, high density lipoproteins; GGE, gradient gel electrophoresis; LCAT, lecithin: cholesterol acyltransferase, EC 2.3.1.43.

<sup>1</sup>To whom communications should be sent, Bowman Gray School of Medicine, 300 South Hawthorne Road, Winston-Salem, NC 27103.

<sup>2</sup>General Clinical Research Center, Francis Scott Key Medical Center, 4940 Eastern Avenue, Baltimore, MD 21224

<sup>3</sup>Donner Laboratory, University of California, Berkeley, CA 94720.

subfraction. Studies using GGE are thus difficult to compare since basic aspects of interpretation of gradient gels vary from laboratory to laboratory. Additionally, these limitations have prevented GGE from being used to quantitatively investigate the metabolic relationships among the various HDL subfractions and between the subfractions and other lipoprotein levels.

## METHODS

Subjects for these studies were from the Baltimore Longitudinal Study of Aging (BLSA), a normative study of men and women who return for followup every 2–3 years. Details of their selection and the measurements performed at each visit have been previously published (12). For these studies, only individuals free of disease and taking no lipid-lowering drugs were studied.

Blood was obtained according to Lipid Research Clinic (LRC) protocol (subject fasting, supine, EDTA anticoagulant) (13). It was immediately centrifuged at 3000 rpm for 30 min at 4°C (DPR-6000, IEC, Austin, TX). For ultracentrifugation at  $d$  1.21 g/ml, 1.0 ml of plasma was mixed with 4.5 ml  $d$  1.254 g/ml KBr, 1 mM EDTA. Ultracentrifugation was carried out in polyallomer heat-sealed tubes, 40,000 rpm, 18–22 h, 5°C (L8-70, 50.3 Ti rotor, Beckman, Fullerton, CA). Floating lipoproteins were recovered by tube slicing after ultracentrifugation, and separated fractions were quantitatively transferred to 2-ml volumetric flasks and adjusted to exact volume with  $d$  1.21 g/ml KBr solution, 1 mM EDTA.

Lipoprotein cholesterol and triglyceride were measured following the LRC protocol (13) with an automatic analyzer (ABA 200, Abbott, North Chicago, IL) and HDL cholesterol was determined after precipitation of other plasma lipoproteins with dextran sulfate–Mg<sup>2+</sup>. The method of Warnick, Benderson, and Albers (3) was used without modification to determine total HDL, HDL<sub>2</sub>, and HDL<sub>3</sub> cholesterol levels. In some experiments, the supernatant solution obtained after precipitation of lipoproteins with dextran sulfate–Mg<sup>2+</sup> was ultracentrifuged at  $d$  1.21 g/ml as described for plasma. Coefficients of variation in measurement were: triglyceride, 4%; cholesterol, 3%; HDL cholesterol, 3%; HDL<sub>3</sub> cholesterol, 8%; and HDL<sub>2</sub> cholesterol, 16%. Triglyceride, cholesterol, and HDL cholesterol standards were traceable to CDC standards.

GGE was performed using nondenaturing 4–30% polyacrylamide gradient gels (PAA 4/30, Pharmacia, Piscataway, NJ) essentially as described by Nichols, Krauss, and Musliner (8). Sample,  $d < 1.21$  g/ml, 100  $\mu$ l, was mixed with 25  $\mu$ l tracking dye solution,  $d$  1.21 g/ml KBr, 1 mM EDTA, 0.25% bromphenol blue (Bio-Rad, Richmond, CA). Ten  $\mu$ l was applied to every other well using a 12-well applicator comb. Wells not containing sample were filled with 10  $\mu$ l  $d$  1.21 g/ml KBr, 1 mM EDTA spa-

cer solution (8). To obtain uniform widths, it was essential to fill wells between samples with spacer solution. Electrophoresis was started for 20 min at 70 V and then continued for 18–24 h at 125 V. Variation in total run times from 16 to 24 h had no effect on separation or measurement of HDL subfractions.

To compensate for gel to gel differences in migration, standards containing thyroglobulin, apoferritin, catalase, lactate dehydrogenase, and bovine serum albumin (Sigma, St. Louis, MO) were run in a separate lane and used to calibrate each gel for determination of the apparent Stokes' radius of subfractions. Hydrated Stokes' radius was used for these calculations: thyroglobulin, 8.5 nm; apoferritin, 6.10 nm; catalase, 5.20 nm; lactate dehydrogenase, 4.08 nm; and bovine serum albumin, 3.55 nm (10). Migration distances were converted to Stokes' radius using the formula derived by Rodbard, Kappadia, and Chrambach (14):  $\log(\text{migration distance}) = A \cdot \log(\text{Stokes' radius}) + B$ . To evaluate use of an internal protein standard to compensate for gel to gel differences in staining, thyroglobulin (Pharmacia, Piscataway, NJ), 1.75 mg/ml was included with the tracking dye in some studies because it migrated to a fixed position above the HDL subfractions. A standard solution of thyroglobulin, 17.5 mg/ml in 0.15 M NaCl, 1 mM EDTA, 3 mM NaN<sub>3</sub> was kept frozen and diluted 1:10 with tracking dye solution immediately before use. For use, 25  $\mu$ l of thyroglobulin standard, diluted with tracking dye, was mixed with 100  $\mu$ l of sample. Because the thyroglobulin contained a contaminant of about 6.5 nm Stokes' radius, no internal standard was added in order to avoid obscuring subfractions near this size during studies of frequency of HDL subfractions.

Gels were fixed and simultaneously stained by soaking overnight in 0.05% Coomassie Blue R-250 (Bio-Rad, Richmond, CA), 9% acetic acid, 20% methanol at room temperature. Stained gels were destained for 24 h at room temperature with two changes of 9% acetic acid, 20% methanol, and finally destained for 48 h with 9% acetic acid. Prolonged destaining with the methanol-containing destaining solution significantly reduced staining intensity. Gels stored in the final 9% acetic acid solution were stable for at least 3 months at room temperature. Gels could be repeatedly stained and destained without measurable change in the proportion of individual subfractions. Use of perchloric acid fixation and Coomassie Blue G-250 staining (8) gave similar results.

Stained gels were scanned using a digital scanning densitometer (Model 620, Bio-Rad, Richmond, CA) equipped with a 600-nm interference filter (Catalog #165-2061, Bio-Rad, Richmond, CA). The interference filter significantly improved the signal to noise ratio. Data from each scan were encoded as the optical density at each pixel (166 pixels/cm), and transferred to an ASCII text file. An interactive computer program was developed using Turbo Basic (Borland, Scotts Valley, CA) to acquire and analyze scan

data. This program is menu-driven and permits: *a*) visualization of the scan, Gaussian model, and difference between model and scan as the scan is analyzed, *b*) scaling and limiting so that only the portion of the scan of interest is displayed, *c*) constant and/or point-to-point subtraction of baseline, *d*) automatic calculation of the results of dropline integration using the cut-points described by Blanche et al. (15), *e*) modelling of the scan data with up to eight Gaussian curves automatically calculating the deviation between data and model and an estimate of goodness of fit (normalized sum of squared derivations), and *f*) optional smoothing. Gaussian curves are specified by moving a cursor that simultaneously displays location, height, and width of the Gaussian. In addition, the program uses data from external standards to automatically calculate the apparent Stokes' radius of the center of each Gaussian curve. The program can also integrate the internal standard area and calculate the amount of each subfraction present in apparent mg protein/ml based on the amount of internal standard or mg cholesterol/dl based on constant or calculated chromogenicities and total HDL cholesterol. Output includes percent of total scan area (OD · mm) and apparent protein (mg/ml) or cholesterol (mg/dl) in each subfraction, peak height (OD), width (mm), and position (mm or calibrated nm), and dropline estimates of percent of total area using the relative mobility ( $R_m$ ) cutpoints described by Blanche et al. (15). Formulae used in this program are given in Appendix 1. An executable copy of this program that runs on most IBM-compatible personal computers is available for noncommercial use from the authors for cost of duplication and postage. Similar results could be obtained with a laser densitometer (UltraScan, LKB, Gaithersburg, MD).

Data were entered into a spreadsheet (Lotus Development, Cambridge, MA) and transferred to a statistical software package (SAS, Cary, NC) for analysis using a personal computer (Premium/286, AST, Irvine, CA) equipped with a math coprocessor (80287, Intel, Hillsboro, OR). Comparisons of methods were made by plotting the differences between results from two methods against the averages of results. The mean difference was considered to be an estimate of the bias between methods, and the 95% confidence interval was calculated as mean  $\pm$  1.96 · standard deviation (16).

## RESULTS

Fig. 1a shows the scan of a typical HDL gradient gel and the six Gaussian curves that best fit the scan. Fig. 1b shows the deviation between scan and the summed Gaussians. In this case, the normalized squared sum of deviations between the original scan and the model,  $Dev^2$ , was 0.07%. Using the computer program described, analysis

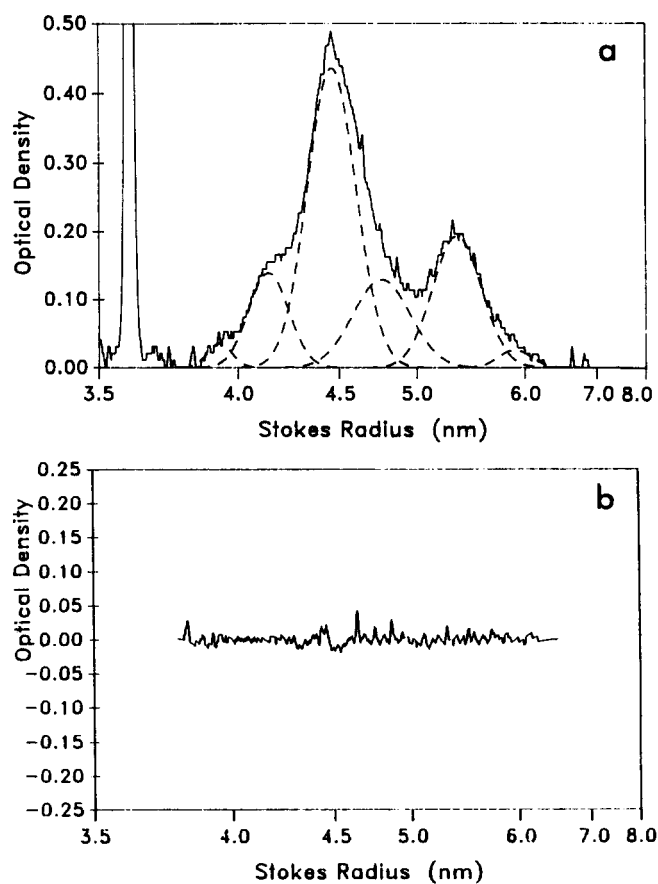


Fig. 1. a: optical density of a stained gradient gel scanned in the HDL region. The solid line shows the original scan, and the dashed line shows the six Gaussian shaped curves that model this scan. Using the nomenclature proposed by Anderson et al. (5), from smallest to largest, the subfractions are HDL<sub>3c</sub>, Stokes' radius 3.9 nm; HDL<sub>3b</sub>, Stokes' radius 4.2 nm; HDL<sub>3a</sub>, Stokes' radius 4.5 nm; HDL<sub>2a</sub>, Stokes' radius 4.8 nm; HDL<sub>2b</sub>, Stokes' radius 5.4 nm; and HDL<sub>1</sub>, Stokes' radius 5.9 nm. Fig. 1b shows the difference between the scan and the model. In this instance the normalized squared deviation was 0.07% of the original HDL area, and the Gaussian curves had a total area of 100.2% of the HDL area.

of a typical scan was accomplished in 5–10 min, giving the height, width, position, and total area of each Gaussian peak needed to model a particular scan. Analysis was considered complete when  $Dev^2$  was minimum and 100% of the scan was modeled with the minimum number of Gaussian curves including at least one curve for each peak and inflection point. Usually, five or six Gaussian peaks, 3.7–6.6 nm Stokes' radius, sufficed to model any HDL pattern with a  $Dev^2 < 0.10\%$  and a Gaussian model equal to  $100 \pm 0.5\%$  of the total area of the scan.

Because the Gaussian curves used to model each scan were individually chosen and optimized by the computer operator, the possibility that different operators might obtain different results was considered. Eight HDL GGE patterns, chosen to include both usual and unusual proportions of subfractions, were analyzed by four different people. Results were compared to estimate the per-

son-to-person coefficient of variation. Between analysts, there was neither significant difference in Stokes' radius of individual peaks (95% confidence interval:  $-0.3$ – $0.2$  nm) nor significant difference in area (95% confidence interval:  $-0.05$ – $1.5$  OD · mm).

The summed Gaussian method was compared in two stages with the dropline analysis method. First, it was determined that the dropline method described by Blanche et al. (15), implemented at the Donner Laboratory, University of California, gave results similar to those obtained by the dropline method implemented in the program developed for these studies. Gels were scanned and analyzed by both the dropline method and the summed Gaussian method and then sent to the University of California, Berkeley, for scanning and analysis. This comparison of two different scanning and software systems, showed an insignificant difference in percent of total area (95% confidence interval:  $-0.7$ – $0.0$  percent total area), demonstrating that the two scanning systems gave essentially the same results with the same gels.

Second, the results of dropline analysis were compared with Gaussian summation analysis. **Fig. 2** shows this comparison for HDL<sub>3a</sub>, the subfraction which usually had the highest concentration. The area, OD · mm, determined by the two methods was correlated with  $R = 0.90$ . However, at low subfraction levels, the dropline method gave higher results than the summed Gaussian method, while at high levels, it gave lower results than the Gaussian method. **Table 1** shows the results of linear regression analyses comparing the two integration methods. Areas determined by the two methods were correlated with  $R \geq 0.90$  for all subfractions except HDL<sub>3b</sub> and HDL<sub>2a</sub>. However, as with HDL<sub>3a</sub>, linear regression showed that, at low levels, the dropline method gave higher levels than the summed Gaussian method, while at high levels, it gave lower levels than the Gaussian method. The difference between the two

TABLE 1. Comparison by linear regression of areas of HDL subfractions determined by dropline and Gaussian analysis

Subfraction	Slope	Intercept	R
HDL <sub>3c</sub>	0.92	0.15	0.90
HDL <sub>3b</sub>	0.75	0.15	0.87
HDL <sub>3a</sub>	0.50	0.78	0.90
HDL <sub>2a</sub>	0.70	0.92	0.56
HDL <sub>2b</sub>	1.09	0.09	0.99

Thirty six individual samples, separated by gradient gel electrophoresis of  $d < 1.21$  g/ml, were analyzed by both the dropline method, using the  $R_m$  cutpoints of Blanche et al. (15), and the Gaussian summation method. Areas of the subfractions were compared by linear regression as illustrated by HDL<sub>3a</sub>, **Fig. 2**. Values given correspond to the equation: (OD · mm by dropline method) = slope · (OD · mm by Gaussian method) + intercept.

integration techniques was greatest for HDL<sub>3b</sub>, HDL<sub>3a</sub>, and HDL<sub>2a</sub>. Thus, choice of analysis technique significantly affected measurement of levels of the overlapping HDL subfractions, HDL<sub>3b</sub>, HDL<sub>3a</sub>, and HDL<sub>2a</sub>.

To determine the range of linearity of the GGE technique, various amounts of lipoproteins,  $d < 1.21$  g/ml, corresponding to 30–100 mg/dl HDL cholesterol were analyzed. Results, **Fig. 3**, showed that the area, OD · mm, of each peak obtained by summed Gaussian analysis varied linearly with the amount of applied sample and the ratio of the area from each subfraction to the total area was independent of the amount applied. There was no indication of nonlinearity in the level of any of the subfractions to over 3.0 OD · mm, establishing a minimum range over which the levels of each subfraction could be accurately measured.

GGE from 37 individuals were analyzed using this method and the frequency of occurrence of HDL subfractions of various Stokes' radii was graphed to determine whether the sizes of subfractions from different people clustered in specific ranges (**Fig. 4**). At least six different ranges of size of HDL subfractions could be identified. In 36/37 individuals, five major subfractions could be identified and measured in 12/37 individuals, an extra subfraction with Stokes' radius larger than HDL<sub>2b</sub>, of about 6.0 nm could also be found; and in 7/37 individuals an extra subfraction was discerned in the size range between HDL<sub>3a</sub> and HDL<sub>2a</sub>. **Table 2** lists the Stokes' radii, mobility relative to albumin,  $R_m$ , and frequency of occurrence of subfractions in these six ranges. Except for slight differences in  $R_m$  defining each range, and the observation that a sixth HDL subfraction could be routinely observed in about 1/3 of individuals, these results confirm the findings of Blanche et al. (15). The nomenclature identifying HDL subfractions as HDL<sub>3c</sub>, HDL<sub>3b</sub>, HDL<sub>3a</sub>, HDL<sub>2a</sub>, HDL<sub>2b</sub>, and HDL<sub>1</sub>, in ascending order of size,  $3.9 \pm 0.04$  nm,  $4.2 \pm 0.04$  nm,  $4.5 \pm 0.04$  nm,  $4.8 \pm 0.07$  nm,  $5.4 \pm 0.09$  nm, and  $6.0 \pm 0.11$  nm Stokes' radius, respectively, similar to that proposed by Anderson et al. (5) has been adopted in this paper.

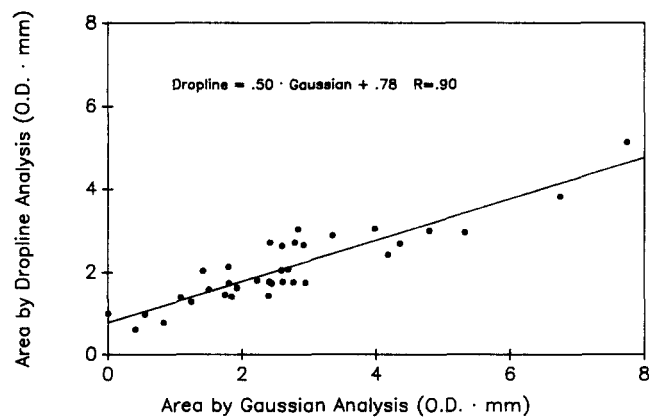


**Fig. 2.** Comparison of areas corresponding to HDL<sub>3a</sub> from 36 GGE scans determined by dropline integration using the cut points of Blanche et al. (15) with those determined by Gaussian analysis. Graphs of the other HDL subfractions were similar and linear analysis of these graphs is in **Table 1**.

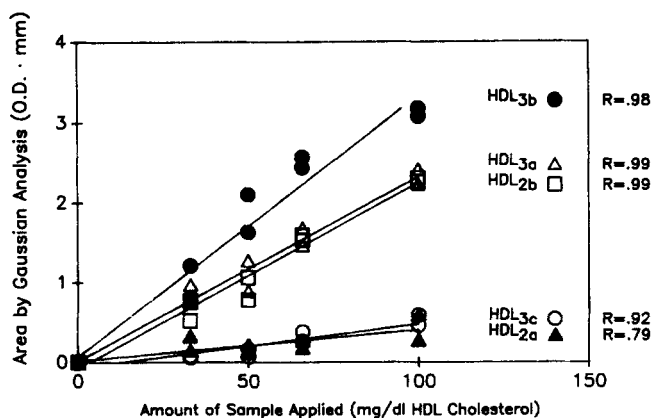


**Fig. 3.** Variation in area of HDL subfractions obtained by Gaussian analysis of duplicate gels with variation in amount of HDL cholesterol applied to the gel. The abscissa is expressed as apparent HDL cholesterol in plasma that would be diluted 1:2.5 as described in the text. Thus, the points at 100 mg/dl were obtained by applying 40  $\mu$ g HDL cholesterol to the gel. Results shown are from one sample of a  $d < 1.21$  g/ml fraction from a woman with relatively high HDL<sub>2b</sub>. Similar linearity was also seen with HDL from a male with less HDL<sub>2b</sub> (not shown). Lines are linear regressions, and results demonstrated linearity to 3.2 OD · mm.

To determine effects of time and condition of storage on measurement of HDL subfractions, after ultracentrifugation, samples were stored at  $-20^{\circ}\text{C}$  and  $4^{\circ}\text{C}$  in d 1.21 g/ml KBr, 1 mM EDTA. Results of preliminary studies (not shown) showed that the HDL subfractions in samples stored at  $4^{\circ}\text{C}$  for up to 60 days varied little in size and showed no significant change in relative amount. When stored at  $-20^{\circ}\text{C}$ , however, significant quantitative and qualitative changes in the HDL subfractions occurred. To obtain more detailed information about changes occurring on storage, samples were stored at  $4^{\circ}\text{C}$  in d 1.21 g/ml KBr for 2 weeks with periodic multiple measurement of subfraction size and quantity. The results of these studies, Table 3, showed that no significant change in size or amount of the most abundant subfractions occurred in 14 days under these conditions, although after 7 days, subfractions amounting to less than 5% of the total were not reliably measured. These repeated measurements of HDL subfractions showed that the reproducibility in measurement of any subfraction was  $\pm 1-2\%$  of the total HDL area, similar to the reproducibility seen when the same gels were scanned and analyzed by the dropline method in different laboratories, with coefficients of variation: HDL<sub>3c</sub>, 11-14%; HDL<sub>3b</sub>, 5-13%; HDL<sub>3a</sub>, 3-4%; HDL<sub>2a</sub>, 14-22%; and HDL<sub>2b</sub>, 2-25%. The subfractions with high coefficients of variation were those with low levels.

To measure the amount of cholesterol in each subfraction, chromogenicities, cholesterol/OD · mm were determined. They were calculated assuming that the cholesterol in each subfraction, e.g., HDL<sub>3c</sub>, was equal to the chromogenicity of that subfraction, e.g.,  $C_{3c}$ , multiplied by

the area in OD · mm of the Gaussian curve corresponding to that subfraction, e.g.,  $A_{3c}$ , i.e.,  $\text{HDL}_{3c} = C_{3c} \cdot A_{3c}$ . Total HDL cholesterol determined by precipitation, HDL<sub>t</sub>, was assumed to equal the sum of subfraction cholesterol levels:  $\text{HDL}_t = \text{HDL}_{3c} + \text{HDL}_{3b} + \text{HDL}_{3a} + \text{HDL}_{2a} + \text{HDL}_{2b} + \text{HDL}_1$ . Thus the equation for HDL<sub>t</sub> in terms of chromogenicities was:  $\text{HDL}_t = C_{3c} \cdot A_{3c} + C_{3b} \cdot A_{3b} + C_{3a} \cdot A_{3a} + C_{2a} \cdot A_{2a} + C_{2b} \cdot A_{2b} + C_1 \cdot A_1$ . Calculation of the chromogenicities from this equation can be illustrated by considering six samples with HDL<sub>t</sub> and areas separately measured. In this case, there would be six equations and six unknown chromogenicities; and the six equations could be solved exactly to obtain the chromogenicities. Considering HDL cholesterol levels and subfraction areas from 64 samples as independent variables and the chromogenicities as dependent variables, multiple linear regression was used to calculate the chromogenicities relative to that of HDL<sub>2b</sub>, Table 4a. The HDL<sub>1</sub> subfraction, which was present in less than 30% of the samples, was less than 1% of the total area, and appeared to be a "tail" of HDL<sub>2b</sub>, was included with HDL<sub>2b</sub> for these calculations. Multiple linear regression, equivalent to finding the five chromogenicities that minimized the variance in fitting the data to the equation:  $\text{HDL}_t = C_{3c} \cdot A_{3c} + C_{3b} \cdot A_{3b} + C_{3a} \cdot A_{3a} + C_{2a} \cdot A_{2a} + C_{2b} \cdot A_{2b}$ , also gave standard errors of the estimates of the chromogenicities.

One source of variance in the chromogenicities was variation in conditions of staining and destaining. Because the amount of dye bound to internal standard reflected the staining and destaining of the whole gel, the chromogenicities were calculated after correcting for area in OD · mm of the internal standard thyroglobulin,  $A_{is}$ , by using HDL<sub>t</sub> and the ratios of subfraction areas to internal standard areas, e.g.,  $A_{3c}/A_{is}$ , as independent variables. Results, Table 4b, showed that this correction

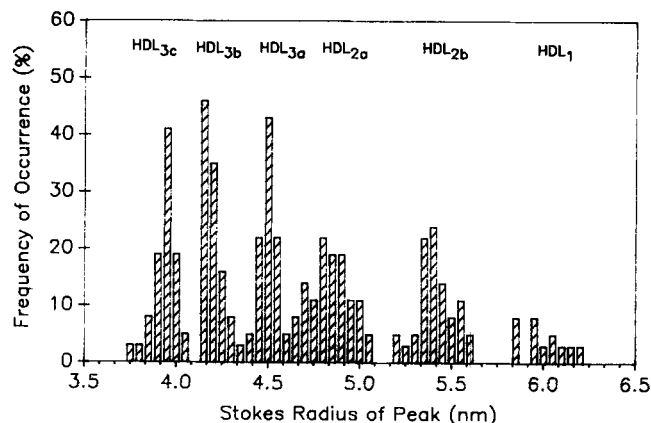


**Fig. 4.** Frequency of occurrence of HDL subfraction peaks of particular Stokes' radius determined by Gaussian analysis of 37 normal HDL samples. Results indicated that five subfractions could be found in 36/37 individuals, consistent with observations of Blanche et al. (15), and that an additional larger subfraction could be found in 12/37 (see text).

TABLE 2. Size ranges of HDL subfractions resolved by Gaussian analysis

Subfraction	n	Mobility Relative to Albumin		Stokes' radius (nm)	
		(Mean)	(Range)	(Mean)	(Range)
HDL <sub>3c</sub>	36	0.88 ± 0.02	0.83-0.93	3.9 ± 0.04	3.77-4.10
HDL <sub>3b</sub>	40	0.81 ± 0.01	0.76-0.83	4.2 ± 0.04	4.10-4.37
HDL <sub>3a</sub>	37	0.73 ± 0.01	0.70-0.76	4.5 ± 0.04	4.37-4.61
HDL <sub>2a</sub>	44	0.66 ± 0.02	0.62-0.70	4.8 ± 0.07	4.61-5.12
HDL <sub>2b</sub>	36	0.57 ± 0.01	0.54-0.62	5.4 ± 0.09	5.12-5.72
HDL <sub>1</sub>	12	0.50 ± 0.02	0.47-0.54	6.0 ± 0.11	5.72-6.58

Mean ± 1 standard deviation of n subfractions detected in 37 scans analyzed, including multiple subfractions in the indicated size range if present (see text).

increased rather than decreased the variance, due to the variability in adding a precise amount of internal standard to each sample and measuring its staining intensity. Thus thyroglobulin internal standard interfered with detecting HDL<sub>1</sub> due to its 6.5 nm Stokes' radius contaminant, and did not contribute to the ability to measure amounts of HDL subfractions.

Since the variance in HDL<sub>t</sub> due to HDL<sub>2b</sub> could be accounted for by measuring HDL<sub>2</sub> using dextran sulfate-Mg<sup>2+</sup> precipitation (see below), chromogenicities, C<sub>3c</sub>, C<sub>3b</sub>, C<sub>3a</sub>, and C<sub>2a</sub>, of the other four subfractions were calculated after subtracting HDL<sub>2</sub> from HDL<sub>t</sub> and A<sub>2b</sub> from the total scan area. These calculations, Table 4c, gave chromogenicities that were similar to those calculated without subtracting HDL<sub>2b</sub> except for C<sub>3b</sub>. The effect of subtracting HDL<sub>2b</sub> from HDL<sub>t</sub> and A<sub>2b</sub> from A<sub>t</sub> on calculation of C<sub>3b</sub> is mathematically due to the apparent physiological correlation between HDL<sub>2b</sub> and HDL<sub>3b</sub>

levels noted below, since effects of variation in A<sub>3b</sub> on the total variance were altered by subtracting the correlated variable, A<sub>2b</sub>. The variance in calculating the chromogenicities also increased due to variability in measuring HDL<sub>2</sub> by precipitation.

Chromogenicities were not statistically different in magnitude and increased from the smallest subfraction, HDL<sub>3c</sub>, to the largest subfractions, HDL<sub>2a</sub> and HDL<sub>2b</sub>, regardless of the independent variables used to calculate them. Linear regression analysis of the chromogenicities in Table 4a showed that the relationship between chromogenicity and Stokes' radius was: chromogenicity (cholesterol/OD · mm) = 0.34 · (Stokes' radius) - 0.75. The standard error of the chromogenicities (coefficient of variation 0.22-0.91) was least for those subfractions present in highest concentration (see below) and the error due to this uncertainty (coefficient of variation multiplied by average concentration was 1.4-4.4 mg/dl, averaging 2.7 mg/dl for

TABLE 3. Changes in HDL subfraction size and quantity with time in storage

Time	Subject #1 (Female)					Subject #2 (Male)				
	HDL <sub>3c</sub>	HDL <sub>3b</sub>	HDL <sub>3a</sub>	HDL <sub>2a</sub>	HDL <sub>2b</sub>	HDL <sub>3c</sub>	HDL <sub>3b</sub>	HDL <sub>3a</sub>	HDL <sub>2a</sub>	HDL <sub>2b</sub>
<i>days</i>	<i>Size (nm)</i>									
1	3.99	4.12	4.59	4.96	5.42	3.98	4.18	4.51	4.82	5.38
4	3.97	4.15	4.52	4.94	5.43	3.92	4.15	4.50	4.93	5.40
7	4.06	4.19	4.53	4.88	5.43	3.86	4.13	4.47	5.10	—
14	4.10	—	4.52	4.52	5.36	3.94	4.17	4.55	5.22	—
Average <sup>a</sup>	4.00	4.16	4.54	4.94	5.42	3.94	4.16	4.51	4.96	5.39
SEM	0.01	0.01	0.01	0.01	0.01	0.01	0.01	0.02	0.06	0.05
	<i>Quantity (fraction of total OD · mm)</i>									
1	0.019	0.045	0.606	0.036	0.294	0.091	0.352	0.370	0.114	0.059
4	0.037	0.052	0.545	0.099	0.267	0.101	0.366	0.405	0.079	0.049
7	0.019	0.050	0.501	0.154	0.276	0.071	0.434	0.457	0.038	<0.010
14	0.011	<0.010	0.628	0.039	0.321	0.052	0.475	0.400	0.075	<0.010
Average <sup>a</sup>	0.027	0.045	0.570	0.076	0.283	0.087	0.384	0.397	0.087	0.040
SEM	0.004	0.006	0.020	0.017	0.007	0.010	0.021	0.017	0.012	0.010

Average of three or four measurements of HDL subfractions stored for indicated times in d 1.21 g/ml KBr at 4°C. These individuals had no HDL<sub>1</sub>. <sup>a</sup>Subject #1, n = 11; subject #2, n = 12.

TABLE 4. Chromogenicities of HDL subfractions relative to HDL<sub>2b</sub>

	HDL <sub>3c</sub>	HDL <sub>3b</sub>	HDL <sub>1a</sub>	HDL <sub>2a</sub>	HDL <sub>2b</sub>
a. Independent variables: total HDL cholesterol (mg/dl) and areas of subfractions (OD · mm), R = 0.96, df = 60					
Chromogenicity	0.59	0.64	0.66	1.12	1.00
SE	0.54	0.35	0.15	0.34	0.22
b. Independent variables: total HDL cholesterol (mg/dl) and ratios of subfraction/internal standard areas, r = 0.91, df = 26					
Chromogenicity	0.03	0.53	0.42	0.53	1.00
SE	0.22	0.32	0.13	0.39	0.29
c. Independent variables: total - HDL <sub>2</sub> cholesterol (mg/dl) and areas of subfractions - HDL <sub>2b</sub> , R = 0.94, df = 60					
Chromogenicity	0.41	0.14	0.81	0.96	1.00
SE	0.17	0.11	0.11	0.08	

Chromogenicities were calculated by multiple linear regression using the indicated independent variables. For these calculations, the chromogenicity of HDL<sub>1</sub> was assumed to be the same as HDL<sub>2b</sub> (see text); R, regression coefficient; df, degrees of freedom; SE, standard error of the individual coefficients.

men and 3.6 mg/dl for women, so the uncertainty in calculating levels of any subfraction due to uncertainty in chromogenicity was 6–7% of total HDL cholesterol.

To quantitatively compare the gradient gel method analyzed by summed Gaussians with the precipitation method of Warnick et al. (3), plasma and supernates obtained after first and second precipitations with dextran sulfate-Mg<sup>2+</sup> were ultracentrifuged at d 1.21 g/ml, and analyzed by GGE using the chromogenicities in Table 4 a. The first supernate purportedly contained the whole HDL fraction and the second, only HDL<sub>3</sub> (3). Results of these analyses, Table 5, showed that the first precipitation removed 94% of the material in the LDL molecular weight range and no significant amount of the HDL<sub>2b</sub>, while the second precipitation removed about 80% of the HDL<sub>2b</sub>. Because some material was left in the LDL region even after two precipitations performed under conditions

known to precipitate all LDL (3), it was assumed that this high molecular weight material was not LDL. It was not further studied. Neither precipitation removed significant amounts of HDL<sub>2a</sub>, so the quantity measured as “HDL<sub>2</sub>” by this precipitation method appeared to be HDL<sub>2b</sub>.

HDL subfraction cholesterol levels were determined in 64 men and women by GGE and analyzed by Gaussian summation using chromogenicities given in Table 4a. Differences between levels of HDL<sub>2b</sub> and HDL<sub>2</sub> were compared with averages of these two measurements, Fig. 5a. The mean difference in levels determined by these two methods was -1.1 mg/dl (standard error = 0.57, 95% confidence interval 0- -2.2 mg/dl). This comparison showed that HDL<sub>2</sub>, measured by dextran sulfate-Mg<sup>2+</sup> precipitation, was statistically equal to HDL<sub>2b</sub> measured by GGE, in agreement with results of ultracentrifugation of supernates obtained after dextran sulfate-Mg<sup>2+</sup> preci-

TABLE 5. Levels of HDL subfractions determined by Gaussian analysis before and after dextran sulfate-Mg<sup>2+</sup> precipitation

Subfraction	Plasma Total	First Supernate	Percent of Plasma Total	Second Supernate	Percent of Plasma Total
	mg/dl			mg/dl	
HDL <sub>3c</sub>	1.2 ± 0.5	1.4 ± 0.5	117	1.4 ± 0.5	117
HDL <sub>3b</sub>	7.3 ± 3.3	6.9 ± 2.9	94	6.1 ± 1.8	84
HDL <sub>3a</sub>	19.0 ± 5.6	20.2 ± 5.2	106	17.9 ± 4.0	94
HDL <sub>2a</sub>	7.6 ± 6.0	7.9 ± 5.5	104	6.1 ± 4.6	80
HDL <sub>2b</sub>	10.2 ± 7.2	9.0 ± 6.6	88	2.4 ± 0.8 <sup>c</sup>	23 <sup>a</sup>
LDL <sup>b</sup>			6 <sup>a</sup>		6 <sup>a</sup>

Mean ± 1 standard deviation of levels and percent of total plasma levels of LDL and HDL subfractions from six individuals, two men and four women. No HDL<sub>1</sub> was measured in these samples.

<sup>a</sup>Statistically significant changes ( $P < 0.05$ ) with precipitation.

<sup>b</sup>LDL estimated as area (OD · mm) of scan in LDL size region. Because independent studies have shown that all LDL was precipitated (3), the 6% of the original area remaining was considered not to be LDL. This material was not studied further.

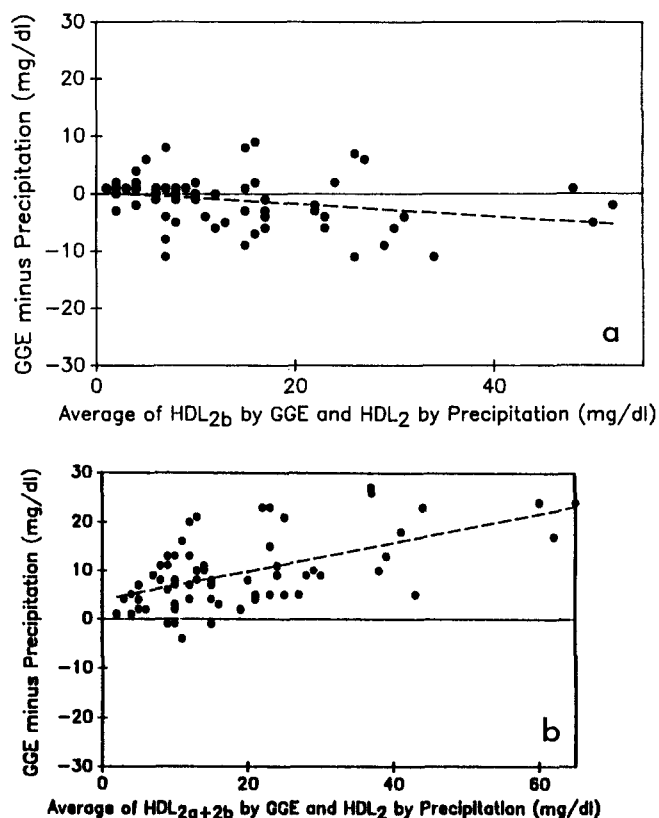


Fig. 5. Graph of differences against averages of levels of HDL<sub>2</sub> determined by dextran sulfate-Mg<sup>2+</sup> precipitation and levels of HDL<sub>2b</sub> (a) and HDL<sub>2a</sub> + HDL<sub>2b</sub> (b) determined by GGE in 64 subjects using the chromogenicities in Table 4a. Dashed lines show the linear regression of differences as a function of averages. The statistically insignificant bias (95% confidence interval 0 to -2.2 mg/dl) between levels of HDL<sub>2</sub> and HDL<sub>2b</sub>, compared with the significant bias (95% confidence interval 7.8-11.4 mg/dl) between levels of HDL<sub>2</sub> and HDL<sub>2a</sub> + HDL<sub>2b</sub>, demonstrated that HDL<sub>2b</sub>, determined using the chromogenicity in Table 4a, equalled HDL<sub>2</sub> by precipitation. This is one demonstration of the validity of using the calculated chromogenicities to measure HDL subfraction levels.

precipitation. In contrast, HDL<sub>2a</sub> + HDL<sub>2b</sub> and HDL<sub>2</sub> were statistically significantly different, bias = 9.6 mg/dl (standard error = 0.93, 95% confidence interval 7.8-11.4), Fig. 5b. These results showed that use of chromogenicity, determined as described above, to measure HDL<sub>2b</sub> levels gave results that were indistinguishable from the precipitation technique, and was therefore valid for measuring this subfraction.

Results of measuring the HDL subfraction levels in these 64 people, Table 6, showed statistically significant differences between men and women in levels of HDL<sub>3a</sub>, HDL<sub>2a</sub>, and HDL<sub>2b</sub>. Although the distribution of samples among different age decades was constant (3-5 men and women per decade), there were too few samples to determine trends related to age. The same measurements were used to determine the correlations among the HDL subfractions and between levels of the subfractions and cholesterol and triglyceride levels, Table 7. These results showed an inverse correlation between levels of HDL<sub>3b</sub> and levels of HDL<sub>2a</sub> and HDL<sub>2b</sub>. They also showed that triglyceride levels were inversely correlated with levels of both HDL<sub>2</sub> subfractions. In addition, they showed that cholesterol levels were directly correlated with levels of HDL<sub>3b</sub> and HDL<sub>3a</sub>. When correlation coefficients were separately calculated, no significant differences between men and women were seen.

## DISCUSSION

In these studies, Gaussian summation analysis of GGE of HDL was developed as a quantitative technique for measuring HDL subfractions with standard errors of repeated measurements of 2% or less of the total HDL area, and accuracy, limited by the standard error of the chromogenicity, of 1-2 mg/dl for the least abundant fractions

TABLE 6. HDL subfraction levels (mg/dl cholesterol) in normal men and women

Subjects	HDL <sub>3c</sub>	HDL <sub>3b</sub>	HDL <sub>3a</sub>	HDL <sub>2a</sub>	HDL <sub>2b</sub>	HDL <sub>1</sub>
Men <sup>a</sup>						
Average	1.5	7.4	14.9 <sup>b</sup>	9.3 <sup>b</sup>	9.0 <sup>b</sup>	0.3
SEM	0.2	0.7	0.9	0.9	1.5	0.5
Range	0-4	1-25	2-25	0-22	1-48	0-2
Women <sup>c</sup>						
Average	2.2	6.9	19.2 <sup>b</sup>	12.8 <sup>b</sup>	18.4 <sup>b</sup>	0.8
SEM	0.5	0.7	1.6	1.5	2.3	0.9
Range	0-16	0-21	0-33	0-29	2-51	0-3

Mean ± 1 standard deviation of age and plasma lipid levels. HDL<sub>1</sub> levels were determined in an unselected subset of 21 men and 13 women assuming chromogenicity equal to HDL<sub>2b</sub>.

<sup>a</sup>Men: n = 36, age 62 ± 15, cholesterol 183 ± 45 mg/dl, triglyceride 108 ± 61 mg/dl.

<sup>b</sup>Significant difference between men and women ( $P < 0.05$ ).

<sup>c</sup>Women: n = 28, age 67 ± 13, cholesterol 195 ± 40 mg/dl, triglyceride 92 ± 42 mg/dl<sup>b</sup>.



TABLE 7. Correlation coefficients between levels of HDL subfractions, plasma triglyceride, and plasma cholesterol

	HDL <sub>1</sub>	HDL <sub>3</sub>	HDL <sub>2</sub>	HDL <sub>3c</sub>	HDL <sub>3b</sub>	HDL <sub>3a</sub>	HDL <sub>2a</sub>	HDL <sub>2b</sub>
TG	-0.40**	NS	-0.45***	NS	NS	NS	-0.43***	-0.44***
Chol	NS	0.44***	NS	NS	0.26*	0.39*	NS	NS
HDL <sub>1</sub>	1	0.70***	0.89***	NS	NS	0.37**	0.62***	0.87***
HDL <sub>3</sub>		1	0.32**	NS	0.36**	0.59***	NS	0.38**
HDL <sub>2</sub>			1	NS	NS	NS	0.68***	0.93***
HDL <sub>3c</sub>				1	NS	NS	NS	NS
HDL <sub>3b</sub>					1	NS	-0.27*	-0.30*
HDL <sub>3a</sub>						1	-0.37**	NS
HDL <sub>2a</sub>							1	0.68***

Correlation coefficients ( $r$ ,  $n = 64$ ) between variables using the same population as in Table 5. When separated into groups of men and women, significant correlations were unchanged. Correlations with HDL<sub>1</sub> were not calculated because of the low level of this subfraction; NS, not significant; \*,  $P < 0.05$ ; \*\*,  $P < 0.01$ ; \*\*\*,  $P < 0.001$ .

and 3–4 mg/dl for the most abundant subfractions. Chromogenicities of the HDL subfractions were determined and used to measure subfraction cholesterol levels in normolipidemic people. These normative values showed differences between men and women in levels of HDL<sub>3a</sub>, HDL<sub>2a</sub>, and HDL<sub>2b</sub>, inverse correlations between levels of HDL<sub>3b</sub> and HDL<sub>2b</sub>, and correlations between levels of specific HDL subfractions and total plasma cholesterol and triglyceride levels. The sum of five or six Gaussian curves typically sufficed to model any HDL scan. Consistent with the studies of Blanche et al. (15), these curves clustered in unique size ranges, although a large HDL subfraction, HDL<sub>1</sub>, was also detected in about 1/3 of the samples. An HDL subfraction of this size has been seen in some nonhuman primates (17) and may be the same as HDL<sub>1</sub> measured by analytic ultracentrifugation (1).

Validity of this method was demonstrated by comparison with the dropline method of Blanche et al. (15), and with the precipitation method of Warnick et al. (3). The Gaussian summation method gave results that were significantly different from those obtained by the dropline integration method for simple reasons. Because use of the dropline method assumed that all lipoproteins observed in a particular range of mobilities corresponded to the same subfraction, levels were inappropriately high by the dropline method in samples with low or absent amounts of a particular subfraction. Similarly, high levels were underestimated because large peaks appeared to “spread out” on a stained gel. Gaussian summation analysis decreased both of these errors.

Reproducibility and accuracy were equal to or greater than reported with other methods for measuring HDL subfractions (1–8). In addition, the computerized method described has several advantages. Compared with methods that measure only HDL<sub>2</sub> and HDL<sub>3</sub>, at least six different subfractions were reliably measured. Compared with the method of Blanche et al. (15), the chromogenicity of each subfraction has been calculated, and levels of the overlapping subfractions, HDL<sub>2a</sub>, HDL<sub>3a</sub>, and HDL<sub>3b</sub>,

were more accurately determined when they were either large or small fractions of total HDL cholesterol. At least 16 samples could be analyzed simultaneously with commercially available electrophoresis apparatus; and control samples were stable for at least 2 weeks. Thus this method of measuring HDL subfractions has been developed to the point of being potentially a clinically useful method.

Distribution of particle size within any subfraction was not necessarily Gaussian in spite of the empiric usefulness of analyzing GGE scans as the sum of Gaussian shaped curves, since distributions of individual standard proteins were nearly Gaussian but were much narrower than those curves describing HDL subfractions (data not shown). The size distribution within HDL subfractions may have arisen from variations in lipid and protein compositions within any one class of subfraction.

In these studies, the chromogenicity, cholesterol/OD·mm, was determined for each subfraction and used to calculate the levels of HDL subfraction cholesterol in plasma although the specific lipid and protein components of the subfractions that became fixed in the polyacrylamide gel and took up stain were unknown. This was consistent with the expectation that specific HDL subfractions had compositions that did not vary significantly from individual to individual although the amounts did vary. Chromogenicity determined in these studies increased with increasing HDL size. This may have been due to differences in composition between subfractions since larger subfractions have been shown to have higher lipid/protein ratios (6). It may also have been due to differences in recovery of the subfractions. Lower rates of destaining at higher polyacrylamide concentrations may also have contributed to the variation in chromogenicity with Stokes' radius since background was often higher in regions of the gel with higher acrylamide concentrations. Chromogenicities were determined from studies of normolipidemic individuals; and they may be different in individuals with hyperlipidemia or unusual HDL structure or composition.

The correlations between HDL<sub>3b</sub> levels and levels of HDL<sub>2a</sub> and HDL<sub>2b</sub> observed in the normative population studied suggested that there may have been a physiological relationship between these subfractions; and the correlation between levels of HDL<sub>3a</sub> and HDL<sub>3b</sub> and total cholesterol levels suggested that these HDL subfractions may have been involved in cholesterol metabolism. GGE of HDL was originally used by John Glomset to study HDL subfractions in LCAT deficiency (10, 11). Since then, it has been used by many investigators to study HDL subfractions before and after affinity chromatography in normolipidemic individuals and subjects with abnormal HDL (15, 18-20). It has been used to determine changes in HDL subfractions caused by diet (21), to identify small HDL subfractions in hypertriglyceridemia (22), and to study effects of LCAT and other agents on HDL structure and composition (10, 11, 23). It has also been used to determine the apparent size of HDL from recombination experiments and the changes in HDL size caused by action of LCAT (24, 25). These quantitative and qualitative observations make it likely that levels of individual HDL subfractions have physiological significance.

Data reported from immunoaffinity column separations of HDL (17) can be interpreted as showing that HDL<sub>2b</sub> and HDL<sub>3b</sub> may have similar apolipoprotein A-I/A-II ratios and it can be hypothesized that apolipoprotein levels may stay constant in individuals while interconversions between HDL subfractions occur due to the action of LCAT, lipoprotein lipase, and/or hepatic lipase (26). Lack of association of triglyceride levels with levels of small HDL<sub>3</sub> subfractions in this normative study is not consistent with increased amounts of small HDL found in hypertriglyceridemia (21), perhaps because increased levels of HDL<sub>3c</sub> in hypertriglyceridemia occurred by a process related to the etiology of the hyperlipidemia that did not occur in normolipidemic individuals. Further studies of the origin, metabolism, and fate of the individual HDL subfractions are needed. ■

#### APPENDIX

Optical density (OD) measurements,  $S_i$ , were made at evenly separated distances,  $X_i$ . Background at each distance,  $B_i$ , was calculated from line segments defined by the investigator. The scan, with background subtracted,  $S_i - B_i$ , was modelled by a sum of Gaussian curves,  $G_k$ , defined at each distance by the equation  $G_{ik} = H_k \cdot \exp - (C_k - X_i)^2/W_k^2$ , with height,  $H_k$  in OD, center,  $C_k$ , in mm, and width,  $W_k$ , in mm. When calibrated using migration distances of standard proteins,  $C_k$  was interpreted as the apparent Stokes' radius of the subfraction. The model was calculated at each point as the sum of the Gaussians,  $M_i = \text{Sum}_k(G_{ik})$ . Deviation between scan (background subtracted) and model was calculated at each point,  $D_i = S_i - B_i - M_i$ ; and, to estimate the goodness of fit of the model to the scan (background subtracted), the quantity,  $\text{Dev}^2 = 100 \cdot \text{Sum}_i(D_i^2)/\text{Sum}_i(S_i - B_i)^2$ , was calculated. This normalized squared deviation equalled 100 when there was no model, and 0 when the model corresponded exactly to the scan. Except when scans had decreased signal/noise ratio,  $\text{Dev}^2 < 0.10$  was

routinely attained by editing the height, width, and center of five or six Gaussian curves. The percentage of the scan accounted for by the model,  $100 \cdot \text{Sum}_i(M_i)/\text{Sum}_i(S_i - B_i)$ , was calculated and adjusted to 100 when editing the Gaussian curves as a second criterion for determining an ideal model. This percentage typically was equal to  $100 \pm 0.5$  when  $\text{Dev}^2 < 0.10$ . The total area of the scan equalled  $\text{Sum}_i(S_i - B_i)$  and the area of each Gaussian was calculated by the formula:  $\pi \cdot H_k \cdot W_k/4$ .

These studies were supported in part by the Laboratory of Clinical Physiology, Division of Metabolism, Reubin Andres, M.D., Director, Gerontology Research Center, NIA, NIH; Johns Hopkins Academic Teaching Nursing Home P01AG04402-05, Francis Scott Key General Clinical Research Center Grant M01-RR02719, and the Department of Medicine, Section on Internal Medicine and Gerontology, Bowman Gray School of Medicine. Special acknowledgement is gratefully made to Reubin Andres, M.D. for his ideas, support, and encouragement. Ellen Rogus, Ph.D., who reviewed the manuscript and made valuable suggestions, and Marilyn Lumpkin and Elizabeth Bannon, who provided excellent technical assistance are also gratefully acknowledged. Marian C. Cheung, Ph.D., provided original gels and data from a laser densitometer for comparison.

Manuscript received 13 December 1988 and in revised form 10 February 1989.

#### REFERENCES

1. DeLalla, O. F., H. A. Elliott, and J. W. Gofman. 1954. Ultracentrifugal studies of high density serum lipoproteins in clinically healthy adults. *Am. J. Physiol.* **179**: 333-337.
2. Gofman, J. W., W. Young, and R. Tandy. 1966. Ischemic heart disease, atherosclerosis, and longevity. *Circulation.* **34**: 679-697.
3. Warnick, G. R., J. M. Benderson, and J. J. Albers. 1982. Quantitation of high-density-lipoprotein subclasses after separation by dextran sulfate and  $\text{Mg}^{2+}$  precipitation. *Clin. Chem.* **28**: 1574.
4. Gidez, L. I., G. J. Miller, M. Burstein, S. Slagle, and H. A. Eder. 1982. Separation and quantitation of subclasses of human plasma high density lipoproteins by a simple precipitation procedure. *J. Lipid Res.* **23**: 1206-1223.
5. Anderson, D. W., A. V. Nichols, T. M. Forte, and F. T. Lindgren. 1977. Particle distribution of human serum high density lipoproteins. *Biochim. Biophys. Acta.* **493**: 55-68.
6. Patsch, W., G. Schonfeld, A. M. Gotto, and J. R. Patsch. 1980. Characterization of human high density lipoproteins by zonal ultracentrifugation. *J. Biol. Chem.* **255**: 3178-3185.
7. Nestruck, A. C., P. D. Niedmann, H. Wieland, and D. Seidel. 1983. Chromatofocusing of human high density lipoproteins and isolation of lipoproteins A and A-I. *Biochim. Biophys. Acta.* **753**: 65-73.
8. Nichols, A. V., R. M. Krauss, and T. A. Musliner. 1986. Nondenaturing polyacrylamide gradient gel electrophoresis. *Methods Enzymol.* **128**: 417-431.
9. Lefevre, M., J. C. Goudey-Lefevre, and P. S. Roheim. 1987. Gradient gel electrophoresis-immunoblot analysis (GGEI): a sensitive method for apolipoprotein profile determinations. *J. Lipid Res.* **28**: 1495-1507.
10. Mitchell, C. D., W. C. King, K. R. Applegate, T. Forte, J. A. Glomset, K. R. Norum, and E. Gjone. 1980. Characterization of apolipoprotein E-rich high density lipoproteins in familial lecithin:cholesterol acyltransferase deficiency. *J. Lipid Res.* **21**: 625-634.

11. Chen, C., K. Applegate, W. C. King, J. A. Glomset, K. R. Norum, and E. Gjone. 1984. A study of the small spherical high density lipoproteins of patients afflicted with familial lecithin:cholesterol acyltransferase deficiency. *J. Lipid Res.* **25**: 269-282.
12. Shock, N. W., R. C. Greulich, R. Andres, D. Arenberg, P. T. Costa, E. G. Lakatta, and J. D. Tobin (editors). 1984. Normal human aging: the Baltimore longitudinal study of aging. National Institute on Aging, NIH, Baltimore, MD. 45-94.
13. Hainline, A., J. Karon, and K. Lippel (editors). 1982. Manual of Laboratory Operations, Lipid Research Clinic Program. National Heart, Lung, and Blood Institute, NIH, Bethesda, MD.
14. Rodbard, D., G. Kappadia, and A. Chrambach. 1971. Pore gradient electrophoresis. *Anal. Biochem.* **40**: 135-157.
15. Blanche, P. J., E. L. Gong, T. M. Forte, and A. V. Nichols. 1981. Characterization of human high-density lipoproteins by gradient gel electrophoresis. *Biochim. Biophys. Acta.* **665**: 408-419.
16. Bland, J. M., and D. G. Altman. 1986. Statistical methods for assessing agreement between two methods of clinical measurement. *Lancet.* **1**: 307-310.
17. Babiak, J., A. V. Nichols, E. L. Gong, C. A. McMahan, T. J. Kuehl, G. E. Mott, and H. C. McGill. 1985. Effects of dietary polyunsaturated and saturated fats on lipoproteins in the baboon. *Atherosclerosis.* **57**: 1-17.
18. Cheung, M. C., and J. J. Albers. 1984. Characterization of lipoprotein particles isolated by immunoaffinity chromatography. *J. Biol. Chem.* **259**: 12201-12209.
19. Carlson, L. A. 1982. Fish eye disease: a new familial condition with massive corneal opacities and dyslipoproteinemia. *Eur. J. Clin. Invest.* **12**: 41-53.
20. Forte, T. M., A. V. Nichols, R. M. Krauss, and R. A. Norum. 1984. Familial apolipoproteins A-I and apolipoprotein C-III deficiency: subclass distribution, composition, and morphology of lipoproteins in a disorder associated with premature atherosclerosis. *J. Clin. Invest.* **74**: 1601-1613.
21. McNerney, C. A., M. L. Kashyap, R. L. Barnhart, and R. L. Jackson. 1985. Comparison of gradient gel electrophoresis and zonal ultracentrifugation for quantitation of high density lipoproteins. *J. Lipid Res.* **26**: 1363-1367.
22. Hopkins, G. J., L. B. F. Chang, and P. J. Barter. 1985. Role of lipid transfers in the formation of a subpopulation of small high density lipoproteins. *J. Lipid Res.* **26**: 218-229.
23. Nichols, A. V., E. L. Gong, and P. J. Blanche. 1981. Interconversion of high density lipoproteins during incubation of human plasma. *Biochem. Biophys. Res. Commun.* **100**: 391-399.
24. Verdery, R. B. 1975. Relipidation of human plasma apolipoproteins with phospholipids. LBL Report 4717. Lawrence Berkeley Laboratory, Berkeley, CA.
25. Nichols, A. V., P. J. Blanche, E. L. Gong, V. G. Shore, and T. M. Forte. 1985. Molecular pathways in the transformation of model discoidal lipoprotein complexes induced by lecithin: cholesterol acyltransferase. *Biochim. Biophys. Acta.* **834**: 285-300.
26. Nikkila, E. A., T. Kuusi, and M-R. Taskinen. 1982. Role of lipoprotein lipase and hepatic endothelial lipase in the metabolism of high density lipoproteins: a novel concept on cholesterol transport in HDL cycle. In *Metabolic Risk Factors in Ischemic Cardiovascular Disease*. L. A. Carlson, and B. Pernow, editors. Raven Press, New York. 205-215.